

**Seasonal logging,  
process response,  
and geomorphic work**

C. H. Mohr et al.

# Seasonal logging, process response, and geomorphic work

C. H. Mohr<sup>1</sup>, A. Zimmermann<sup>1</sup>, O. Korup<sup>1</sup>, A. Iroumé<sup>2</sup>, T. Francke<sup>1</sup>, and A. Bronstert<sup>1</sup>

<sup>1</sup>Institute of Earth and Environmental Science, University of Potsdam, Potsdam, Germany

<sup>2</sup>Faculty of Forest Sciences and Natural Resources, Universidad Austral de Chile, Valdivia, Chile

Received: 9 July 2013 – Accepted: 3 September 2013 – Published: 5 September 2013

Correspondence to: C. H. Mohr (cmohr@uni-potsdam.de)

Published by Copernicus Publications on behalf of the European Geosciences Union.

Title Page

Abstract

Introduction

Conclusions

References

Tables

Figures

⏪

⏩

◀

▶

Back

Close

Full Screen / Esc

Printer-friendly Version

Interactive Discussion



## Abstract

Deforestation is a prominent anthropogenic cause of erosive overland flow and slope instability, boosting rates of soil erosion and concomitant sediment flux. Conventional methods of gauging or estimating post-logging sediment flux focus on annual timescales, but potentially overlook important geomorphic responses on shorter time scales immediately following timber harvest. Sediments fluxes are commonly estimated from linear regression of intermittent measurements of water and sediment discharge using sediment rating curves (SRCs). However, these often unsatisfactorily reproduce non-linear effects such as discharge-load hystereses. We resolve such important dynamics from non-parametric Quantile Regression Forests (QRF) of high-frequency (3 min) measurements of stream discharge and sediment concentrations in similar-sized ( $\sim 0.1 \text{ km}^2$ ) forested Chilean catchments that were logged during either the rainy or the dry season. The method of QRF builds on the Random Forest (RF) algorithm, and combines quantile regression with repeated random sub-sampling of both cases and predictors. The algorithm belongs to the family of decision-tree classifiers, which allow quantifying relevant predictors in high-dimensional parameter space. We find that, where no logging occurred,  $\sim 80\%$  of the total sediment load was transported during rare but high magnitude runoff events during only 5% of the monitoring period. The variability of sediment flux of these rare events spans four orders of magnitude. In particular dry-season logging dampened the role of these rare, extreme sediment-transport events by increasing load efficiency during more moderate events. We show that QRFs outperforms traditional SRCs in terms of accurately simulating short-term dynamics of sediment flux, and conclude that QRF may reliably support forest management recommendations by providing robust simulations of post-logging response of water and sediment discharge at high temporal resolution.

## Seasonal logging, process response, and geomorphic work

C. H. Mohr et al.

Title Page

Abstract

Introduction

Conclusions

References

Tables

Figures



Back

Close

Full Screen / Esc

Printer-friendly Version

Interactive Discussion



## 1 Introduction

Despite the on-going discussion of whether man-made forests are more prone to soil erosion than native forests or protect degraded soils from erosion instead, reported increases of soil erosion following timber harvest remain undisputed (Gomi et al., 2005; Sidle et al., 2006). Such major impacts occur during, and a few years after, harvesting operations, before the vegetation re-establishes, and road surfaces and embankments stabilize. Clear cutting may intensify erosive overland flow (Malmer and Grip, 1990), trigger landslides along road cuts (Montgomery et al., 2000), or cause debris flows, and river-bank erosion (Gomi et al., 2004), eventually resulting in infrequent sediment pulses. Thus boosted erosion and re-deposition of soil promote the long-term decay of soil conservation functions not only on harvest patches, but also often in downstream areas (Sidle et al., 2006).

Clear cutting is the most common technique of harvesting timber in the plantation forests of Chile. The nation is currently intensifying and extending its forestry sector, and recent projections point to increasing growth rates of timber and cellulose production (FAO, 2010), and an exacerbation of soil erosion in the future. Yet the forestry sector provides a major income source and thus requires a comprehensive assessment of the economic, social, and ecological benefits of forestry. Reliable knowledge of pre- and post-disturbance sediment fluxes is vital in this regard, and may be acquired by physics-based modelling or statistical treatment of field data. Chilean law mandates immediate replantation after clear cutting, thus limiting the time for sampling hydrogeomorphic impacts of clear cutting such that field data may not represent the full range of water and sediment fluxes. This drawback requires a data analysis technique capable of dealing with few samples of high variance under changing environmental conditions (Fig. 1a).

Conventional sediment rating curves (SRCs) rely on an empirical relationship between water discharge and suspended sediment concentration (SSC), but are prone to high uncertainty where SSC-discharge dynamics are subject to disturbances or

# ESURFD

1, 311–335, 2013

## Seasonal logging, process response, and geomorphic work

C. H. Mohr et al.

Title Page

Abstract

Introduction

Conclusions

References

Tables

Figures



Back

Close

Full Screen / Esc

Printer-friendly Version

Interactive Discussion





on top of schist bedrock (Mohr et al., 2012). The climate is Mediterranean, and rainfall intensities are low and do not exceed  $10 \text{ mm h}^{-1}$  in average. Intense convective storms are extremely rare. Previous work shows that only 5% of the registered rainfall events exceed  $23 \text{ mm h}^{-1}$  (Mohr et al., 2013).

Two catchments previously planted with *Pinus radiata* were logged by the same clear-cutting technique during different seasons: catchment #3 was clear cut during the winter rainy season (July–August 2009), and remained bare for  $\sim 1$  yr (Fig. 2a), whereas catchment #4 was harvested during the dry summer season (February 2010), and reforested shortly after. The clear cut was done using heavy rubber-tired skidders to drag logs uphill to landings whereas cable logging was limited to steep slopes (Mohr et al., 2013) (Fig. 2b). Catchment #1 remained unlogged and covered with *P. radiata*, and served as a control catchment. On 27 February 2010, the study area was hit by the *M*8.8 Maule earthquake that caused ground shaking for 2.5 min at ground accelerations of  $\sim 0.3$  g. The regional hydrological response featured an abrupt drop in stream discharge followed by a rapid increase (Mohr et al., 2012).

### 3 Methods

#### 3.1 Field sampling

We measured stream discharge with V-notch Thompson gauges equipped with custom-built water-stage recorders at a frequency of 3 min, and a water-level accuracy of 2 mm (Huber et al., 2010; Mohr et al., 2012, 2013). To the best of our knowledge, such high temporal resolution is unique among similar monitoring studies. Rainfall was recorded by a Hobo tipping bucket with resolution of 0.2 mm. Hourly rainfall intensities were statistically tested using a Wilcoxon rank sum test at the 5%-significance level to test for differences between both studied years. Bulk monitoring data of sediment fluxes from June 2008 to September 2009 in these and adjacent catchments indicate that pine plantations were more prone to soil erosion than eucalyptus plantations

**Seasonal logging,  
process response,  
and geomorphic work**

C. H. Mohr et al.

Title Page

Abstract

Introduction

Conclusions

References

Tables

Figures

◀

▶

◀

▶

Back

Close

Full Screen / Esc

Printer-friendly Version

Interactive Discussion



(Huber et al., 2010). With bed load being negligible in the coastal mountains (Iroumé, 1992), i.e. < 1 % of the total load (A. Huber and C. H. Mohr, unpublished data), we acquired high-frequency data on instantaneous SSC from June 2009 to August 2010 in order to quantify sediment flux in response to logging activities. We sampled SSC on an event basis with an electric pump armed on a floating device submerging the pump aperture at a constant depth of 5 cm below the water surface in the weirs. We took instantaneous SSC samples on an event basis at 30 to 60 min intervals (Fig. 2c). In the absence of significant rainfall events, we took at least one complementary daily sample during February/March, and August 2010 for characterizing low-flow conditions (Table 1). All SSC samples were then rounded to the next 3 min interval to synchronize with discharge measurements. SSC were determined gravimetrically with an accuracy of 0.5 mg after filtering the runoff samples (Mohr et al., 2013). We obtained sediment yields by multiplying the SSC with the runoff volume summed over the respective time intervals

$$SSY = \int_{t1}^{t2} Q(t) SSC(t) \quad (1)$$

where SSY is suspended sediment yield ( $g s^{-1}$ ),  $Q$  is instantaneous discharge ( $L s^{-1}$ ), and SSC is instantaneous sediment concentration ( $g L^{-1}$ ).

We complemented this event-based sampling by monitoring suspended sediment flux with weekly volume weighted bulk sampling (Huber et al., 2010) (Fig. 2c). Despite larger sampling intervals, this alternative monitoring scheme provided data without the need to interpolate SSC. We considered these data as first-order benchmarks for the modelled sediment fluxes. To obtain representative and homogeneous integrated samples, the pump sampled water volumes that are always directly scaled to water stage with higher discharge contributing commensurately more than lower water stages. Any integrated sample merged four samples each day over a period of one week (Huber

**Seasonal logging,  
process response,  
and geomorphic work**

C. H. Mohr et al.

Title Page

Abstract

Introduction

Conclusions

References

Tables

Figures

◀

▶

◀

▶

Back

Close

Full Screen / Esc

Printer-friendly Version

Interactive Discussion



et al., 2010). The sediment yields were then estimated following Eq. (1) as previously described.

### 3.2 Sediment Rating Curve (SRC)

For each catchment, we fitted sediment rating curves to a power-law function relating SSC values to the correlate discharge  $Q$  (e.g., Gomi et al., 2005)

$$SSC = a Q^b, \quad (2)$$

where  $a$  ( $g s^b L^{-(b+1)}$ ) and  $b$  are empirical fitting parameters of log-transformed data. Based on the SRC, we predicted SSC during the study period and performed the same 20-fold cross validation procedure as described for QRF (see Sect. 3.3).

### 3.3 Quantile Regression Forests (QRF)

Quantile Regression Forests (QRF) is a robust non-parametric regression technique (Meinshausen, 2006) that builds on Random Forest (RF) regression tree ensembles, a data mining method based on the repeated random selection of both training data and predictors (Breiman, 2001). QRF is a generalization of the RF algorithm. For each node in each tree, RFs calculate the mean of the observations that are split along this node. RF does not consider further information, whereas QRF considers the full distribution of all tree predictions (Meinshausen, 2006), thus quantifying inherent uncertainties of each model (Zimmermann et al., 2012). This step is needed for estimating prediction intervals, which encompass new observations with high likelihood. Both the RF and QRF algorithms also help to incorporate effects of variable interaction, and offer means of quantifying relative variable importance (Francke et al., 2008a; Zimmermann et al., 2012) by assessing the decline in model performance due to randomizing predictor variables during each iteration.

Title Page

Abstract

Introduction

Conclusions

References

Tables

Figures

◀

▶

◀

▶

Back

Close

Full Screen / Esc

Printer-friendly Version

Interactive Discussion



### 3.4 QRF model

We set up individual QRF models for each catchment to predict SSC from the (a) rainfall and discharge time series; (b) day of year to account for possible seasonality effects; and (c) change in discharge to capture dynamics between events (Francke et al., 2008a). We quantified antecedent hydro-meteorological conditions by computing predictor variables that integrated antecedent rainfall and discharge values over multiples of the sampling interval. Time interval and number of aggregation levels were set to 3 and 6, respectively. These settings describe the successive increase of aggregation windows into the past and their total number in the generation of the aggregated predictors. For example,  $P_{28-81}$  refers to the rainfall accumulated between 28 and 81 min prior to a given SSC sample (Zimmermann et al., 2012). In order to prevent collinearity, overlaps between each window were avoided (Zimmermann et al., 2012). We added counter variables starting at the time of clear cutting to capture possible effects of timber harvest and vegetation recovery over time to involve changing environmental conditions. We further defined a switch variable that stratified the data into pre- and post-seismic periods for identify potential earthquake impacts (Supplement Table S1).

We assessed the relative predictor importance based on permutation (Strobl et al., 2008). This measure accounts for multi-collinearity and associated overestimation of variable importance due to spurious correlation artefacts (Liaw and Wiener, 2002). We validated model performance applying the root mean square error

$$\text{RMSE} = \sqrt{\frac{1}{N} \sum_{i=1}^N (x_i - \hat{x}_i)^2} \quad (3)$$

for  $N$  measurements  $x_i$ , and predictions  $\hat{x}_i$ . In order to avoid arbitrary decisions during the validation procedure, e.g. size and location of the test data set, we applied a 20-fold cross validation leaving out continuous data blocks of 5 % of the data to test the models, respectively (Zimmermann et al., 2012). We defined 10 % of the SSC range ( $\text{g L}^{-1}$ ) as a threshold range for acceptable model performance accounting for the distinct parameter range of measured SSC, and inherent erosion modeling limitations. Such limitations

Title Page

Abstract

Introduction

Conclusions

References

Tables

Figures

◀

▶

◀

▶

Back

Close

Full Screen / Esc

Printer-friendly Version

Interactive Discussion



arise from unavoidable bias due to the random component of all measured data feeding any erosion model (Nearing, 1998). Finally, we estimated suspended sediment yields for each 3 min time step applying a Monte Carlo simulation (Francke et al., 2008a). To this end we randomly drew a SSC prediction from the distribution realized by the QRF model for each time step. Based on these samples, we estimated event dynamics and both monthly and annual sediment yields by summing up the products of  $Q$  and SSC at each time step over each target period. By repeating this procedure 250 times, we obtained a distribution of SSY estimates which was then checked for Gaussian shape. The latter allowed us to calculate their mean value and standard deviation to assess the spread of the predicted sediment yields (Zimmermann et al., 2012).

## 4 Results

Compared to the traditional sediment-rating curve approach, QRF predicted SSC with high accuracy under both low- and high-flow regimes, as well as unlogged and logged conditions. Figure 3 illustrates the predictive accuracy for high SSC under disturbed conditions, and the additional advantage of QRF to compensate for poor, or impute missing, rainfall and discharge data (Fig. 7a–c). The method also reproduced hysteresis loops, and the occurrence of multiple peak events (Fig. 3). Treating errors  $< 10\%$  of the measured SSC range as acceptable, both QRF and SRC met this criterion across all catchments (Supplement Table S2). Yet QRF generally outperformed SRC except for rainy-season logging where the large range of measured SSC values shrunk relative differences in model performance to  $< 1\%$ .

We compared monthly and annual specific suspended sediment yields (SSY) predicted from both QRF and SRC with the bulk data, using a Monte Carlo simulation (Francke et al., 2008a) (Supplement Tables 3–5). Specific sediment yield averaged for the first two years following rainy-season logging was  $3.27 \pm 0.09 \text{ t ha}^{-1}$  or  $\sim 20$  times the SSY predicted for unlogged conditions ( $0.19 \pm 0.004 \text{ t ha}^{-1}$ ;  $\pm 1\sigma$ ). However, monthly SSY from the catchment planned to be harvested during rainy season exceeded that

## Seasonal logging, process response, and geomorphic work

C. H. Mohr et al.

Title Page

Abstract

Introduction

Conclusions

References

Tables

Figures



Back

Close

Full Screen / Esc

Printer-friendly Version

Interactive Discussion



## Seasonal logging, process response, and geomorphic work

C. H. Mohr et al.

Title Page

Abstract

Introduction

Conclusions

References

Tables

Figures



Back

Close

Full Screen / Esc

Printer-friendly Version

Interactive Discussion



in the unlogged control catchment by a factor of  $\sim 5$  even before logging commenced (Fig. 4a). Similarly, the catchment that was subjected to dry-season logging yielded  $\sim 4$  times the SSY of the control catchment before it was clear cut (Fig. 4b). The decreasing slope of the double-mass curve after dry-season logging indicates that soil erosion intensified over undisturbed conditions only after rainy-season logging.

When normalized to the increase under unlogged control conditions, SSYs increased from 2009 to 2010 by  $\sim 125\%$  following rainy-season logging, but decreased by  $\sim 40\%$  after dry-season logging. This finding is in line with our bulk data measurements (Supplement Table S3). Overall, QRF predicted substantially higher sediment yields than the SRC approach. Only for undisturbed conditions and dry-season logging were SRC predictions within the same order of magnitude. Based on bulk data, SRC underestimates annual SSY by a factor of 2–28 (Supplement Table S3), despite overestimating sediment flux during individual peak runoff events (Figs. 3, 7).

Our QRF-derived estimates show that, under unlogged conditions,  $\sim 80\%$  of the total sediment load carried during the monitoring period was transported during only  $\sim 5\%$  of the time. Most of the sediment was transported during rare, large runoff events. The instantaneous flux rate ( $\text{g s}^{-1}$ ) variability of these rare events spanned four orders of magnitude, and thus more than the variability of all other rates occurring over 95% of the monitoring period (Fig. 5a). Our QRF data thus indicate that logging, regardless of its seasonal timing, coincided with a relatively increased contribution of moderate as opposed to extreme runoff events in terms of sediment transport. Thus, immediate post-logging effects on sediment transport involved the reduction of sediment transport during peak flow events while shifting the geomorphic work towards less flashy and more moderate events. We found this effect to be more pronounced for dry-season than for rainy-season logging (Fig. 5b).

To rank the contributions of different environmental controls as predictors of sediment flux we quantified their relative importance in terms of added total predictive accuracy (Fig. 6). We found that antecedent rainfall accumulated 28 to 81 min prior to a given SSC sample was most influential for unlogged conditions, whereas the timing of logging



## Seasonal logging, process response, and geomorphic work

C. H. Mohr et al.

Title Page

Abstract

Introduction

Conclusions

References

Tables

Figures



Back

Close

Full Screen / Esc

Printer-friendly Version

Interactive Discussion



events. Our results significantly expand down to the process time scale the notion that extreme sediment transport events may perform the bulk of geomorphic work (Korup, 2012). Our findings also underscore the impact that logging may have on shifting the underlying frequency-magnitude distributions of water and sediment flux (Fig. 5). We interpret these as statistically robust changes, given that QRF avoids over-fitting by randomly selecting both data and predictor subsets, while providing objective measures of their relative importance (Fig. 6). Predictor importance also changes as a function of the logging season. The resulting predictions are not only in line with the base flow-dominated discharge, but also maintain low uncertainty because of the averaging out of low-precision predictions (Zimmermann et al., 2012). Nevertheless, QRF may have drawbacks for high magnitude rainfall-runoff events (Fig. 7d–f) given the method’s inability to extrapolate beyond the parameter space, and especially the monitoring period. Seasonal effects may not be fully represented in the time series (Fig. 6) because our observation windows in time have significantly different rainfall patterns (Supplement Table S4). Our study area is dominated by frontal rainfall events instead of high-intensity convective storms, and we caution against extrapolating our results for rainfall-runoff events of higher magnitude. In essence, QRF is a robust and versatile method for hindcasting high-frequency time series of water and sediment discharge, but not designed for predicting future events.

Compared with similar studies on logging effects (e.g., Gomi et al., 2005), our QRF predictions indicate very low to even slightly decreasing post-logging sediment yields following dry-season logging when compared to unlogged conditions. Our observation of increased post-rainy-season logging sediment flux is consistent with previous work (e.g., Sidle et al., 2006). Yet the magnitude of this increase is small (e.g., Gomi et al., 2004), and our SSY estimates are within the range reported for natural, undisturbed forests (Zimmermann et al., 2012). The observed decreases of SSY following dry logging (Fig. 4b) may partly be due to prompt replanting of the logged slopes (Malmer and Grip, 1990). Some maintenance works on a timber road in 2010 in the unlogged catchment are also likely to have contributed to elevating the local sediment supply

given that unsealed timber roads may dominate sediment production per unit area in managed forests (e.g., Motha et al., 2003). Consequently, we expect that the thus elevated sediment flux in the unlogged catchment may have partly smothered the relative impact of logging in the other catchments.

We also exclude seasonal meteorological differences as drivers of the elevated SSYs in 2010, as rainfall was much higher in 2009 at comparable intensities (Supplement Table S3). Moreover, the timing of the 2010 earthquake did not notably distort any of the SSC predictions (Fig. 6) despite favourable conditions for post-seismic increases in sediment flux (Hovius et al., 2011). The limited earthquake response may be linked to a decisive lack of post-seismic rainfall in 2010, which may have otherwise triggered mass wasting. Plantations of *P. radiata* are prone to mass wasting because of their low root-strength compared with other species (Watson et al., 1999). When logged, they rapidly decay in root-strength (Sidle, 1991). Shallow landslides are also promoted by slow root-strength recovery rates and cumulative effects of preceding rotations (Sidle et al., 2006). Given that root decay and regrowth have opposite trends over time, we expect maximum mass wasting rates 2–3 yr after logging (Watson et al., 1999). Hence, our immediate post-logging predictions of SSC (Fig. 6) are consistent with mechanistic slope-stability models (Sidle et al., 2006). During the monitoring period of this study, however, we regard the contribution of mass wasting processes as minor, and hitherto insufficient, for explaining the hydro-geomorphic post-logging regimes.

The QRF-derived variable importance plot supports the notion of a predominant overland flow mechanism of recent harvest areas (Fig. 6). Infiltration capacity may increase on recently logged areas, thus impeding infiltration-excess overland flow generation under the low rainfall intensities observed (Mohr et al., 2013). Alternatively, high-duration rainfall is required to elevate groundwater levels, which in turn initiate erosive saturation-excess overland flow (Dunne and Black, 1970), and connect sediment sources to the drainage network. The relevance of several antecedent rainfall characteristics for predicting post-logging sediment fluxes reflects the local rainfall regime, where low-intensity and long-duration rainfall events successively saturate the

## Seasonal logging, process response, and geomorphic work

C. H. Mohr et al.

Title Page

Abstract

Introduction

Conclusions

References

Tables

Figures



Back

Close

Full Screen / Esc

Printer-friendly Version

Interactive Discussion



soil layers over time, thus permitting erosive overland flow (Huber et al., 2010). Compared with rainy-season logging, the measured SSC following dry-season logging also responded to significantly longer time lags. The lower cohesion of wet soil elevates sediment supply for erosive overland flow during timber machinery action in the rainy season. Hence, the susceptibility to soil erosion is higher compared to logging in dry soil conditions. The distinct micro-topography left by heavy machinery persisted following dry-season logging until the subsequent rainy season, thus impeding overland-flow connectivity, and requiring larger volumes of water to re-establish connectivity (Mohr et al., 2013). In contrast, SSC under unlogged conditions appears to be modified by more short-term antecedent rainfall characteristics (Fig. 6). Such flashiness may indicate effects of hydrophobic plantation forest cover (e.g., Miyata et al., 2009).

## 6 Conclusions

Our study provides novel insights into the immediate hydro-geomorphic process response to different seasonal timber harvest operations. We find that Quantile Regression Forests (QRF) outperform sediment rating curves (SRC) in terms of accurately predicting post-logging sediment yields at the process scale. Using empirical sediment rating curves may lead to grave underestimates of sediment fluxes from managed forests. Our unprecedented high-frequency data on post-logging water and sediment fluxes from three Chilean headwater basins corroborates the widely held view that most sediment transport is accomplished within a few rare high-discharge events, particularly at the timescale of immediate hydro-geomorphic process response. Moreover, QRF-based hindcasting underlines that it is the seasonal timing of clear cutting that dictates the amount of shift in the frequency-magnitude relationship of sediment transport, eventually redistributing geomorphic work from rare, extreme events to more moderate ones. Dry-season logging led to a much higher dampening of extreme events, whereas rainy-season logging accentuated the contrasts in instantaneous transport

**Seasonal logging,  
process response,  
and geomorphic work**

C. H. Mohr et al.

Title Page

Abstract

Introduction

Conclusions

References

Tables

Figures



Back

Close

Full Screen / Esc

Printer-friendly Version

Interactive Discussion



rates. Post-logging increases in sediment flux, most likely driven by saturation-excess overland flow, were an order of magnitude higher following rainy-season clear cutting.

Our work motivates further testing of whether QRF are suitable tools for longer-term time series, thus allowing direct comparison with studies that recorded the annual to decadal net effects of logging and hydro-geomorphic recovery. Still, given that data scarcity and variability are common for post-logging disturbances, we find that Quantile Regression Forests turns out to be a robust and promising tool for quantifying in detail high-frequency time series of water and sediment fluxes following clear-cut operations.

**Supplementary material related to this article is available online at**  
[http://www.earth-surf-dynam-discuss.net/1/311/2013/  
esurfd-1-311-2013-supplement.pdf](http://www.earth-surf-dynam-discuss.net/1/311/2013/esurfd-1-311-2013-supplement.pdf).

*Acknowledgements.* We thank Andreas Bauer, Johannes Brenner, Franziska Faul, Rodrigo Bravo and Cristian Frêne Conget for helping in field and during data analysis. We are grateful to Forestal Mininco for providing access to our experimental catchments, and acknowledge Anton Huber for support and advice. This study is co-funded by the International Bureau of the German Federal Ministry of Education and Research and the Chilean Government (CONICYT/BMBF 2009-092 and 2010-243).

## References

- Asselman, N. E. M.: Fitting and interpretation of sediment rating curves, *J. Hydrol*, 234, 228–248, doi:10.1016/S0022-1694(00)00253-5, 2000.
- Breiman, L.: Random forests, *Mach. Learn.*, 45, 5–32, doi:10.1023/A:1010933404324, 2001.
- Dunne, T. and Black, R. D.: An Experimental investigation of runoff production in permeable soils, *Water Resour. Res.*, 6, 478–490, doi:10.1029/WR006i002p00478, 1970.
- FAO: Global Forest Resources Assessment 2010, Main Report, Food and Agriculture Organization of the United Nations, Rome, 2010.

**Seasonal logging,  
process response,  
and geomorphic work**

C. H. Mohr et al.

Title Page

Abstract

Introduction

Conclusions

References

Tables

Figures



Back

Close

Full Screen / Esc

Printer-friendly Version

Interactive Discussion



## Seasonal logging, process response, and geomorphic work

C. H. Mohr et al.

Title Page

Abstract

Introduction

Conclusions

References

Tables

Figures

◀

▶

◀

▶

Back

Close

Full Screen / Esc

Printer-friendly Version

Interactive Discussion



Francke, T., Lopez-Tarazon, J. A., and Schroder, B.: Estimation of suspended sediment concentration and yield using linear models, random forests and quantile regression forests, *Hydrol. Process.*, 22, 4892–4904, doi:10.1002/hyp.7110, 2008a.

5 Francke, T., Lopez-Tarazon, J. A., Vericat, D., Bronstert, A., and Batalla, R. J.: Flood-based analysis of high-magnitude sediment transport using a non-parametric method, *Earth Surf. Proc. Land.*, 33, 2064–2077, doi:10.1002/esp.1654, 2008b.

Gomi, T., Sidle, R. C., and Swanston, D. N.: Hydrogeomorphic linkages of sediment transport in headwater streams, Maybeso Experimental Forest, southeast Alaska, *Hydrol. Process.*, 18, 667–683, doi:10.1002/hyp.1366, 2004.

10 Gomi, T., Moore, R. D., and Hassan, M. A.: Suspended sediment dynamics in small forest streams of the Pacific Northwest, *J. Am. Water Resour. Assoc.*, 41, 877–898, doi:10.1111/j.1752-1688.2005.tb03775.x, 2005.

Hovius, N., Meunier, P., Lin, C.-W., Chen, H., Chen, Y.-G., Dadson, S., Horng, M.-J., and Lines, M.: Prolonged seismically induced erosion and the mass balance of a large earthquake, *Earth Planet. Sc. Lett.*, 304, 347–355, doi:10.1016/j.epsl.2011.02.005, 2011.

15 Huber, A., Iroumé, A., Mohr, C. H., and Frene, C.: Effect of *Pinus radiata* and *Eucalyptus globulus* plantations on water resource in the Coastal Range of Biobio region, Chile, *Bosque*, 31, 219–230, 2010.

Iroumé, A.: Precipitación, escorrentía y producción de sedimentos en suspensión en una cuenca cercana a Valdivia, Chile, *Bosque*, 13, 15–23, 1992.

20 Korup, O.: Earth's portfolio of extreme sediment transport events, *Earth-Sci. Rev.*, 112, 115–125, 2012.

Liaw, A. and Wiener, M.: Classification and Regression by randomForest, *R News*, 2, 18–22, 2002.

25 Malmer, A. and Grip, H.: Soil disturbance and loss of infiltrability caused by mechanized and manual extraction of tropical rain-forest in Sabah, Malaysia, *Forest Ecol. Manag.*, 38, 1–12, doi:10.1016/0378-1127(90)90081-L, 1990.

Meinshausen, N.: Quantile regression forests, *J. Mach. Learn. Res.*, 7, 983–999, 2006.

Miyata, S., Kosugi, K., Gomi, T., and Mizuyama, T.: Effects of forest floor coverage on overland flow and soil erosion on hillslopes in Japanese cypress plantation forests, *Water Resour. Res.*, 45, W06402, doi:10.1029/2008WR007270, 2009.

30 Mohr, C. H., Montgomery, D. R., Huber, A., Bronstert, A., and Iroumé, A.: Streamflow response in small upland catchments in the Chilean coastal range to the M-W 8.8 Maule earthquake on



## Seasonal logging, process response, and geomorphic work

C. H. Mohr et al.

Title Page

Abstract

Introduction

Conclusions

References

Tables

Figures

◀

▶

◀

▶

Back

Close

Full Screen / Esc

Printer-friendly Version

Interactive Discussion



**Table 1.** Number of total samples for each catchment. Sample size of pre-logging period given in brackets.

Catchment	Sample number $n$	Start date	End date
#1	278	06/27/2009	08/15/2010
#3	276 ( $n_{\text{pre}} = 89$ )	06/27/2009	08/29/2010
#4	100 ( $n_{\text{pre}} = 24$ )	02/19/2010	08/28/2010

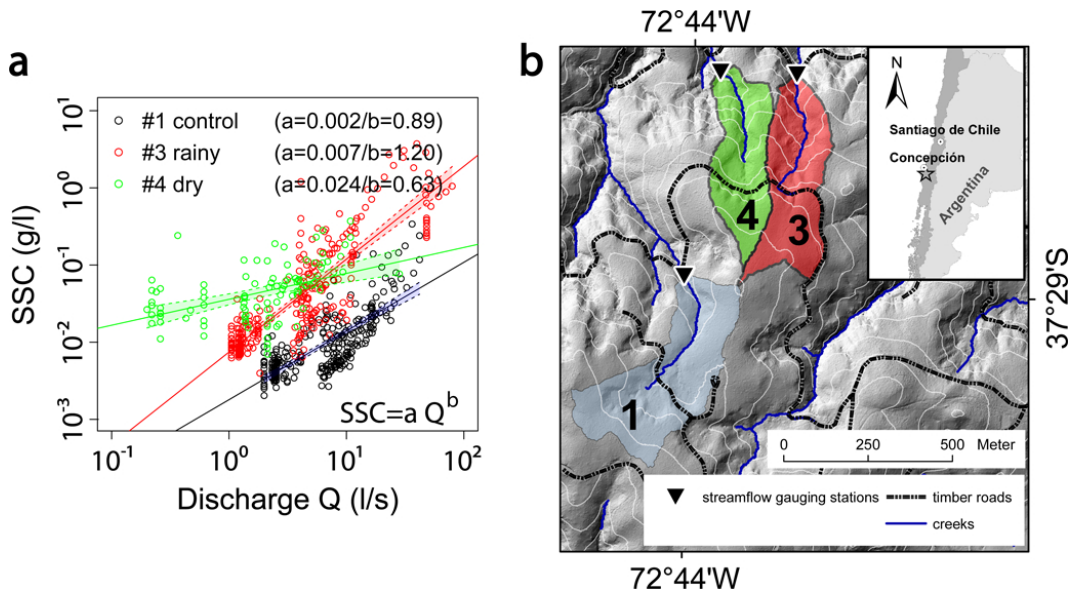


**Fig. 1. (a)** Sediment rating curves for the catchments with fitted power-law intercepts  $a$  ( $g s^b L^{-(b+1)}$ ), slopes  $b$ , and 95%-confidence intervals about regression lines. **(b)** Location of study catchments (star in inset) including stream gauges; and unpaved timber roads. Topography derived from LiDAR survey; contour spacing is 20 m. Numbers (consistent with previous work) refer to catchments. See Huber et al. (2010), Mohr et al. (2012) and (2013) for detailed descriptions of these catchments.

**Seasonal logging,  
process response,  
and geomorphic work**

C. H. Mohr et al.

Title Page

Abstract Introduction

Conclusions References

Tables Figures

◀ ▶

◀ ▶

Back Close

Full Screen / Esc

Printer-friendly Version

Interactive Discussion





**Fig. 2.** Pictures showing the experimental catchments, the logging procedure and the suspended sediment monitoring devices. **(a)** Rainy season logged watershed (watershed #3) in the subsequent dry season (March 2010); **(b)** Skidder dragging logged stems uphill to the next landing in watershed #3; **(c)** Custom-built sediment sampling system: (1) horizontal rotating table used to sample suspended sediment on event-base; (2) recipient used to collect bulk sample of suspended sediment on weekly base.

## Seasonal logging, process response, and geomorphic work

C. H. Mohr et al.

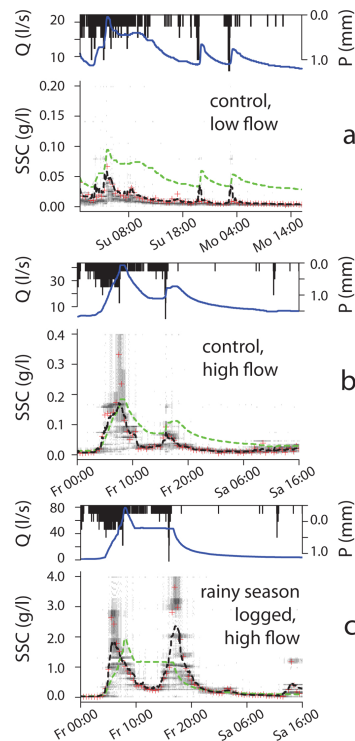


**Fig. 3.** Water discharge and SSC dynamics under unlogged and logged conditions during two rainfall events. **(a)** 27–29 June 2009, catchment #1; **(b–c)** 14–15 August 2009, catchments #1 and #3. Density of SSC predictions of the QRF model for each time step encoded by SSC in grey histograms; black dashed lines are means of these predictions; red crosses are measured SSC; green dashed lines are SSC predictions of the SRC. Data are from calibration period, i.e. periods are covered with SSC samples used for model building (see Fig. 7 for limits to model predictions).

Title Page

Abstract

Introduction

Conclusions

References

Tables

Figures

◀

▶

◀

▶

Back

Close

Full Screen / Esc

Printer-friendly Version

Interactive Discussion



## Seasonal logging, process response, and geomorphic work

C. H. Mohr et al.

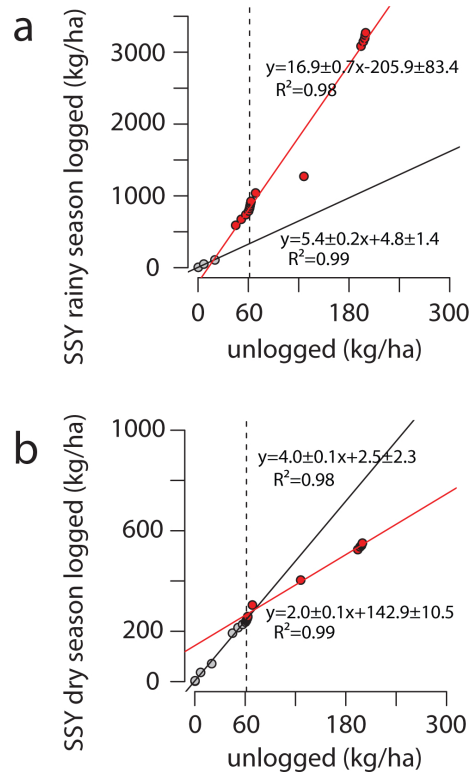


**Fig. 4.** Monthly double mass-curve analysis between the sediment yields (SSY) of catchments logged during **(a)** rainy and **(b)** dry season, and the unlogged control catchment. Black vertical dashed line separates 2009 and 2010 study periods; grey and red circles are pre- and post-logging sediment yields, respectively; lines are best-fit linear regression models. Uncertainties are  $\pm 1$  standard deviations.

Title Page

Abstract

Introduction

Conclusions

References

Tables

Figures

◀

▶

◀

▶

Back

Close

Full Screen / Esc

Printer-friendly Version

Interactive Discussion

## Seasonal logging, process response, and geomorphic work

C. H. Mohr et al.

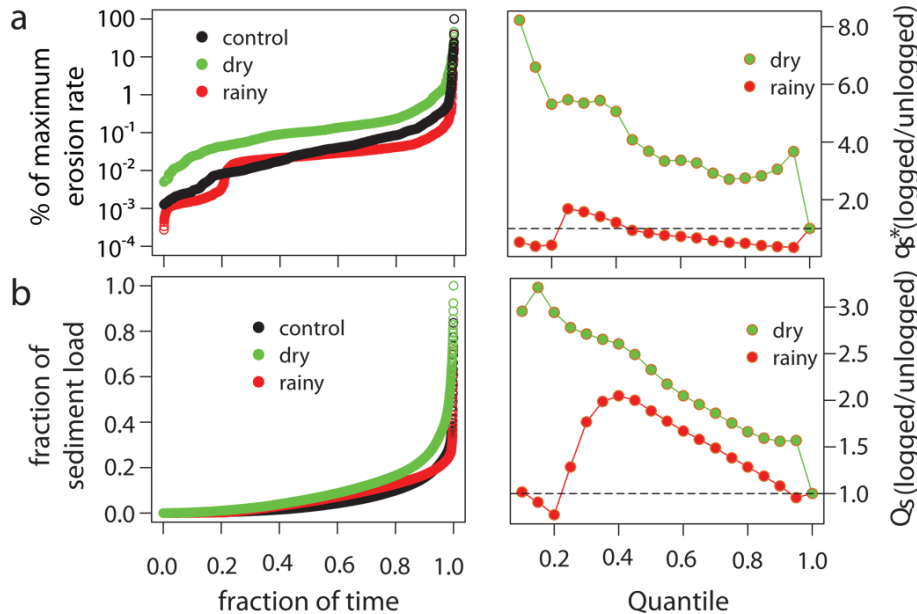


**Fig. 5.** (a) Fraction of instantaneous sediment transport rates normalized to catchment maximum as a function of monitoring time during which these rates were not exceeded. (b) Fraction of total sediment load normalized per catchment as a function of the fraction of total monitoring period for unlogged conditions, rainy-, and dry-season logging. Right-hand panels show resulting ratios of instantaneous transport rates  $q_s^*$ , and total sediment loads  $Q_s$  per quantile for logged versus unlogged conditions. Black vertical dashed lines are 1 : 1 ratio. Empirical cumulative distribution functions differ significantly ( $p < 0.01$ ; Kolmogorov-Smirnov test).

## Seasonal logging, process response, and geomorphic work

C. H. Mohr et al.

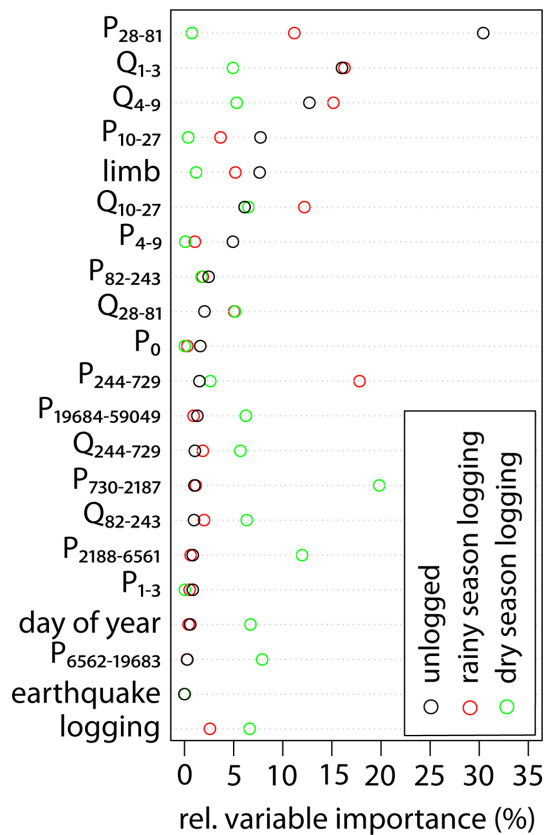


**Fig. 6.** Variable importance of the Quantile Regression models for each catchment scaled to 100 % in order to facilitate inter-catchment comparison. See Supplement Table S1 for predictor variables.

Title Page

Abstract Introduction

Conclusions References

Tables Figures

◀ ▶

◀ ▶

Back Close

Full Screen / Esc

Printer-friendly Version

Interactive Discussion



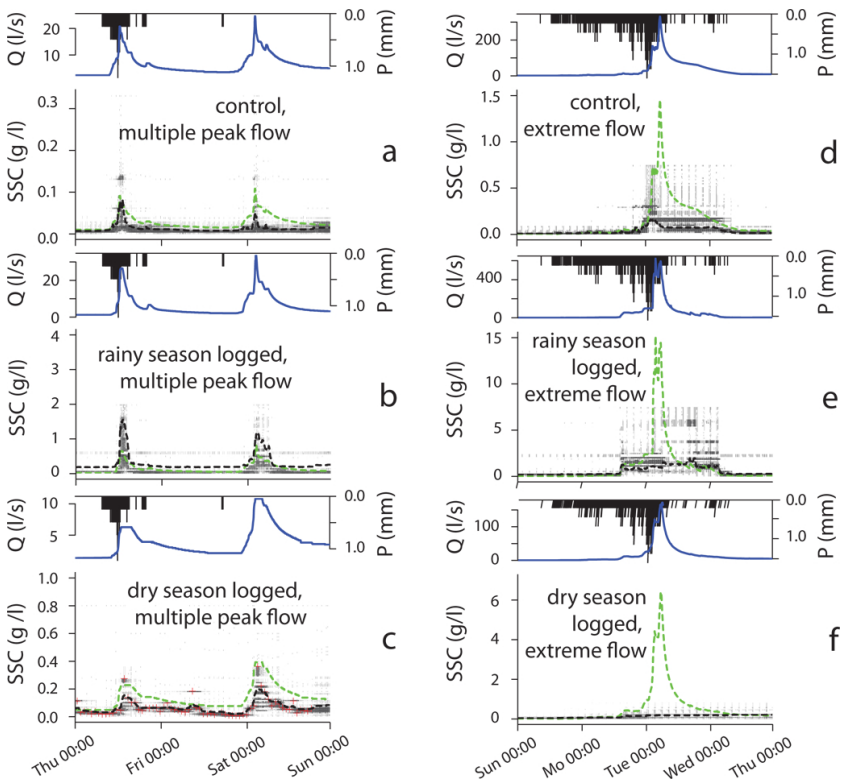


**Fig. 7.** QRF model results of SSC dynamics during extreme peak flow for undisturbed and logged conditions during two rainfall events, i.e. 15–18 August 2010 (**a–c**) and 26–28 August 2010 (**d–f**). Density of SSC predictions of the QRF model for each time step encoded by grey histograms; black dashed lines are means of these predictions; red crosses are measured SSC; green dashed lines are SSC predictions based on SRCs.